THE USE OF STORAGE RINGS IN THE STUDY OF REACTIONS AT LOW-MOMENTUM TRANSFERS*

Nasser Kalantar-Nayestanaki

for the EXL Collaboration

KVI-CART, University of Groningen, Groningen, The Netherlands

A few aspects of the nucleus manifest themselves in direct reactions where the transferred momentum to the nucleus is very small. In the study of radioactive isotopes, one has to use inverse kinematics in which the radioactive ion impinges on a stable target. When the momentum transfer is low, one has to do these reactions with either an active target or in a storage-ring environment. In this contribution, the latter method will be discussed in some detail as the active targets are discussed in other contributions. The pilot studies performed by the EXL Collaboration in 2012 lead to the first ever measurements of reactions employing radioactive isotopes in the ring. In this contribution, the first results will be presented. The outlook will indicate in which directions the future of this field will be headed.

1. Introduction

In the study of the structure of nuclei, one has to perform measurements in a large range of momentum transfers in order to fully understand the details. However, the experimental conditions for low-momentum- and high-momentum-transfer measurements are quite different. Since all studies of interest will be carried out in inverse kinematics, a low-momentum-transfer measurement necessitates the utilization of storage rings due to very small recoil energies. These low-energy particles would simply be stopped in any external target. The alternative would be to use active targets but that will only be suitable for low luminosities. One should then perform these measurements in internal-target facilities in which the target thickness must

---

* Presented at the Zakopane Conference on Nuclear Physics "Extremes of the Nuclear Landscape", Zakopane, Poland, August 28–September 4, 2016.

be very small to allow the passage of low-energy particles and, at the same time, maintain a reasonable life-time for the circulating beam. The very small target thicknesses used in the rings are compensated for by circulating the beam in the ring a couple of million times a second, thereby, increasing the effective luminosity, making the in-ring experiments comparable to external-target measurements as far as the luminosity is concerned. In addition, the large momentum spread and the large emittance of the beam coming from the FRagment Separator (FRS at GSI or Super-FRS at the future FAIR facility [1]) should be reduced in order to achieve the goals of the low-momentum-transfer measurements. This is done by cooling the beam in the storage ring. One clear advantage of performing the experiments in the storage ring is the lack of background from the target windows which are present in the external-target experiments. The high-momentum-transfer measurements, on the other hand, do not suffer from the above-mentioned energy limitations and as such are better carried out in external-target facilities. The intensity of the beams delivered from FRS or Super-FRS could, in fact, be low, since the required luminosity can be obtained by making the target thicker. To this end, the compromise between the energies of the outgoing particles, their required resolutions and the cross sections of a given reaction determine what target thickness one can use. In short, one would need a storage ring to perform the low-momentum-transfer measurements and an external target for the high-momentum-transfer measurements. The experiments EXL (EXotic nuclei studied in Light-ion induced reactions at a storage ring) [2], shown in Fig. 1 and R^3B (Reactions with Relativistic Radioactive Beams), placed in the high-energy branch of the FAIR facility [3], are designed to address these two aspects and are, in that sense, completely complementary to each other.

The key physics issues being covered with the EXL (and R^3B for the high-momentum transfer measurements) program are:

— nuclear matter distributions near the drip lines. The halo structures as well as the nuclear skins will be thoroughly studied;

— new collective modes (different deformations for protons and neutrons), giant and pygmy resonances with different multipolarities;

— parameters of nuclear equation of state;

— the isospin-dependence of the single-particle shell structures (new magic numbers, new shell gaps and spectroscopic factors);

— nucleon–nucleon correlations and cluster formation;

— in-medium interactions in asymmetric and low-density nuclear matter;

— the astrophysical r- and rp-processes in the form of Gamow–Teller transitions, neutron capture, *etc.*
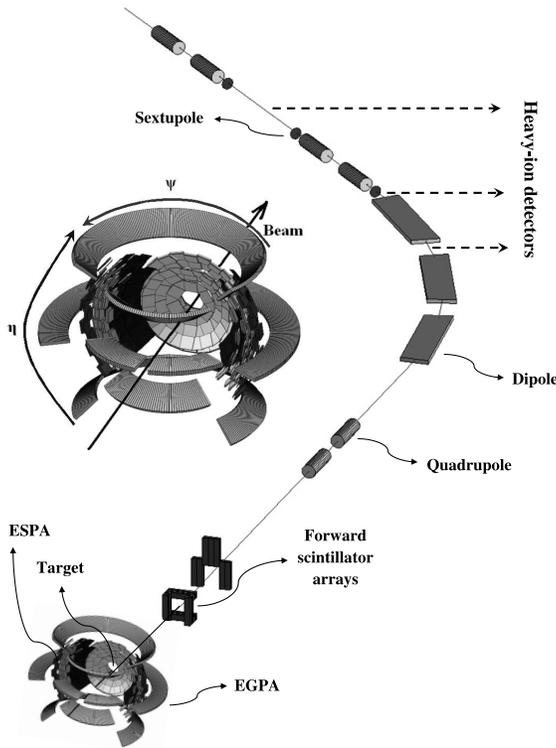
Fig. 1. The overview of the EXL setup with various components shown. The recoil detector is enlarged and shown in the middle. Note that only a few rings of the calorimeter and some segments of the Si array are drawn here for the sake of clarity.

All these studies can be done in the light-ion induced direct reactions, such as elastic (p, p), (α, α) scattering, inelastic scattering in (p, p'), (α, α'), charge-exchange reactions of the type (p, n) or $(^3\text{He}, t)$, and $(d, ^2\text{He})$, quasi-free scattering like $(p, 2p)$, (p, pn), and $(p, p+\text{cluster})$ and, finally, the transfer reactions of the type (p, t), $(p, ^3\text{He})$, (p, d), and (d, p). The relevant information should be extracted from an energy and momentum measurement of the outgoing particles. In these experiments, it should be possible to detect many of the outgoing particles, making most of the channels kinematically (over)complete. This is particularly necessary in reducing the backgrounds in measurements when the cross sections are very low. As an example, with elastic proton scattering from a radioactive isotope and, in particular, at low-momentum transfers, one can deduce the matter-density distribution. This, combined with electron scattering on the same object (*á la* ELectron-Ion Scattering in a storage ring, ELISe [4]) will result in neutron density distributions.

2. EXL setup

Within the EXL Technical Proposal [2], the design of a complex detection system was investigated with the aim to provide a high-efficiency, high-resolution, and a universal setup, applicable to a wide class of reactions (see Fig. 1). The apparatus is foreseen to be installed around the internal target position of one of the storage rings at the future FAIR facility. The detection system includes:

— Si-strip and thick Si(Li) detectors (ESPA) for recoiling target-like reaction products, completed by slow-neutron detectors (not shown in the figure), and a calorimeter (EGPA) with a high granularity for γ rays and for the total-energy measurement of more energetic target recoils;

— detectors in forward direction (schematically shown in the figure as forward scintillator arrays) for fast ejectiles from the excited projectiles, *i.e.* neutrons and light charged particles;

— heavy-ion detectors for the detection of beam-like reaction products.

All detector components will practically cover the full relevant solid angle and have detection efficiencies close to unity. With this setup, kinematically-complete measurements will become possible.

Major research and development work was required for the design and the technical implementation of the target-recoil detector which is the most challenging part of the project. In particular, the detector components need to fulfil strong demands concerning angular and energy resolutions, detection thresholds, dynamic range, granularity, ultra-high vacuum compatibility, *etc.*, partly not available or derivable from the existing detection technologies. A second major task is to achieve high densities in the internal gas-jet target, of the order of 10^{14}–10^{15} atoms/cm^2 or above with a well-localized interaction zone [5]. On both fronts, there have been major developments going on with very promising results. In 2005 and 2011, feasibility measurements in the present Experimental Storage Ring (ESR) at GSI were performed with a small number of detectors representing various components of the EXL detection system [6–10]. These included a Si-strip detector placed in vacuum, plastic scintillators to detect the fast forward recoil particles, and a combination of a p-i-n diode and a scintillator placed after the first bending magnet to detect the projectile-like heavy ions. The results of both measurements were very promising and paved the way for the final design of the first setup explained in the next section and which was used in the physics experiment.

3. EXL prototype setup for the 1st reaction experiment at a ring

Based on the results of the first test measurements, prototyping of various components, and specially those which had to operate under the ultra-high vacuum condition were done successfully [11–13]. For the first time, an experiment (E105) was performed with a radioactive beam interacting with a light nucleus in an storage ring with the aim of obtaining physics results. For this experiment which was done in 2012, ^{56}Ni was the chosen beam. This nucleus has several features making it very attractive to study. It is a doubly magic unstable nucleus with a long life-time (~ 6 days) which is an advantage for storage-ring environment. In addition, it is a waiting point nucleus in the r-process which occurs in the formation of stars.

The existing storage ring ESR at GSI was used for these measurements. The ESR has a circumference of 108.4 m and a maximal magnetic rigidity of 10 Tm. The quality of the beam was improved by both stochastic and electron cooling. After cooling, the momentum spread is of the order of $\delta p/p \approx 10^{-5}$ [14]. The operation of a storage ring requires an Ultra-High Vacuum (UHV) better than 10^{-10} mbar which imposes a major challenge on experiments performed in the ring. In the experiment reported here, the stored beam impinged on an internal gas-jet target of H_2 or He [15].

As mentioned above, the main challenge in the low-q measurements in inverse kinematics is the detection of very low-energy recoil particles. For this purpose, window-less and highly-segmented Si strip detectors capable of operating under UHV were developed [12, 13]. In our design, these detectors serve both as detectors and active windows separating the UHV of the storage ring from the auxiliary vacuum in a pocket which accommodates the non-bakeable parts of the system (see Fig. 2). In order to achieve the UHV conditions, the Double-sided Si Strip Detectors (DSSDs) were mounted on ceramic AlN boards, a material which is non-outgassing and bakeable. Figure 2 shows the experimental setup used in our experiment with the two detectors mounted in the scattering chamber which was placed in the ESR.

The first detector, labelled 1st DSSD in the figure, consists of a 6×6 cm^2 DSSD of 285 μm thickness with 128×64 segments followed by two 8×4 cm^2 Si(Li) detectors of 6.5 mm thickness with 4×2 segments. The Si(Li)s were equipped with a cooling system to keep their temperature low even during the baking of the pocket. This detector was centered at 80.5° in the laboratory system. The second detector, labelled 2nd DSSD in the figure, consisted only of a DSSD of the same type and was centred at 32.5°.

The production of ^{56}Ni beam was done by the fragmentation of a primary beam of ^{58}Ni in the FRagment Separator (FRS) at GSI. This resulted in an intensity of about 4×10^4 ^{56}Ni ions of 400 MeV/nucleon per spil. Several injections and stacking [16] in the ESR were required to obtain the desired
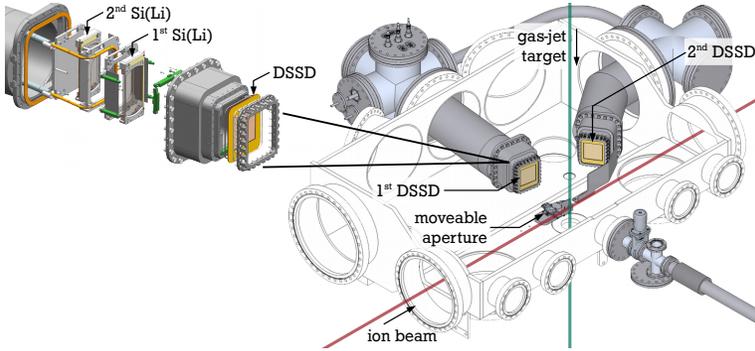
Fig. 2. The detection setup as used in the ESR ring for the pilot experiments. Two DSSDs along with the moveable aperture are shown. The directions of the beam and the gas-jet target are also indicated in the figure.

intensity of about 3×10^6 ions circulating in the ring with a frequency of about 2 MHz. The life-time of the circulating beam in the ring was about 1.5 hours. This, coupled to a H_2 gas-jet target density of about $3 \times 10^{13}/\text{cm}^2$ resulted in a peak luminosity of about $2 \times 10^{26}/\text{cm}^2/\text{s}$. With this intensity, the first ever measurements for the elastic scattering of protons from ^{56}Ni could be performed with a few days of beam-time.
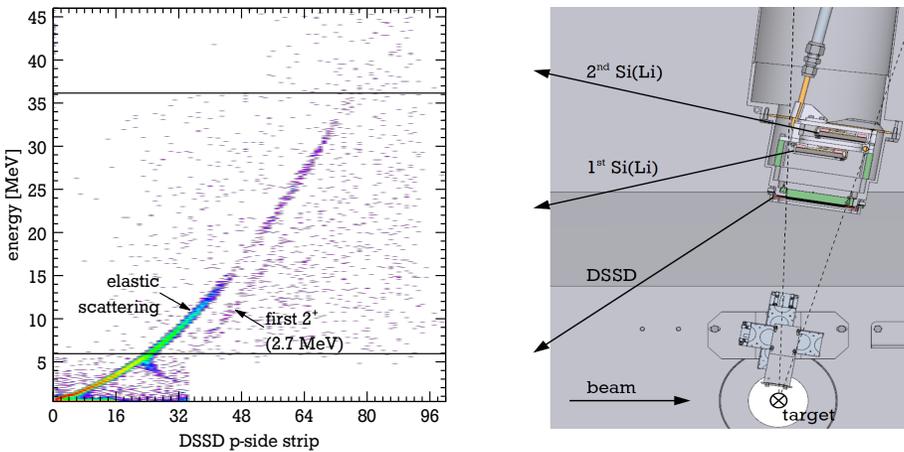

Fig. 3. Reconstructed laboratory energies of the recoiling protons after scattering from ^{56}Ni. The reconstructed energy is the sum of all the deposited energies in the first DSSD and the two Si(Li) detectors behind it. Note that the punch-through point for the first DSSD is about 6 MeV and that for the first Si(Li) is about 36 MeV (indicated by lines).

These first measurements suffered from the finite size of the beam and the target. In our measurement, we have a reasonable beam with the size of about $\sigma = 0.6$ mm. However, the target size which was about 3.2 mm in radius posed a serious limitation in the angular resolution of the measurements. This would, in turn, hinder the separation of the first excited state of ^{56}Ni at 2.7 MeV from the ground state. To overcome this problem, a moveable aperture was installed between the target and the first DSSD and as close as possible to the target (see Fig. 2). Only with this slit, which also limited the luminosity of the experiment, it was possible to have a clear separation between the ground and the first excited state (see Fig. 3).

4. First physics results

4.1. Proton elastic scattering from ^{56}Ni

From the number of counts in each strip and after the proper energy and angle calibrations, cross sections were obtained for the elastic scattering of protons from ^{56}Ni. For this, the 1$^{\text{st}}$ DSSD was used which covers angles close to 90° in the laboratory frame. This angle corresponds to 0° in the center-of-mass (CM) frame for elastic scattering. The results are shown in Fig. 4 along with the results of a fit using Glauber multiple-scattering theory and a matter distribution with a symmetric Fermi function. From this, an RMS matter radius can be obtained. The elastic scattering cross-section data for ^{58}Ni were used in connection with published results for this nucleus to fix some parameters of the model [17]. With this, the procedures for obtaining density parameters were thoroughly checked.
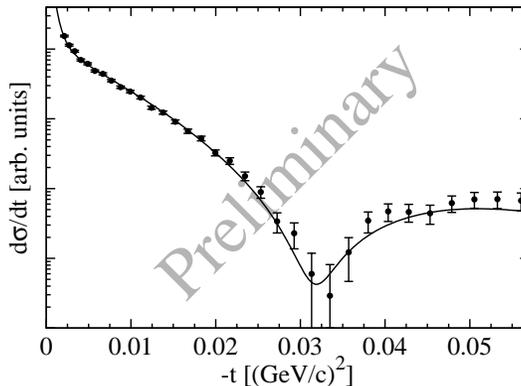

Fig. 4. Shown is a fraction of the data obtained for the experimental cross section of the elastic proton scattering from ^{56}Ni at an incident energy of 400 MeV/nucleon. The errors are primarily statistical. The curve represents a fit to the data using Glauber multiple-scattering theory.

The preliminary value of the RMS (folded) matter radius lies in the range of 3.7–3.8 fm with an expected uncertainty of the order of 0.1 fm [18] which is in the range of most theoretical predictions [19, 20] while it rules out the lower values predicted by [21].

4.2. Isoscalar Giant Monopole Resonance in ^{58}Ni

The 2nd DSSD was placed in the scattering chamber to cover forward angles (at a central value of 32.5°). These angles correspond to very small CM angle for excitation energies around 20 MeV which is roughly where the peak of the IsoScalar Giant Monopole Resonance (ISGMR) would be. For this experiment which should be preferably performed with an isoscalar probe, a gas-jet target of ^{4}He with a density of about $2 \times 10^{12}/cm^2$ was employed. Since the intensity of ^{56}Ni was not sufficient to obtain results with reasonable statistics within a reasonable time, the decision was made to use the primary ^{58}Ni beams with much higher intensities for this measurement.

The challenge for these measurements is that although the cross section increases with incident-beam energy, the energy of the recoiling particle decreases making it impossible to detect them. A compromise energy of 100 MeV/nucleon was chosen for this experiment resulting in outgoing recoil energies of a few hundreds keV.

Figure 5 shows a typical energy spectrum of one of the strips. One can clearly see the effect of δ-electrons which have a maximum energy of around 200 keV. With the help of simulations, this physical background can be sub-
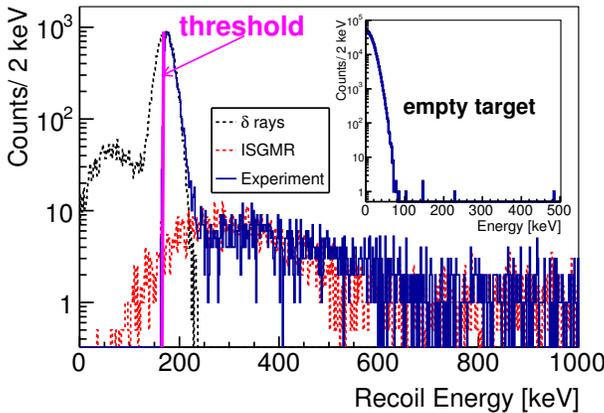

Fig. 5. Energy spectrum of one of the detector strips positioned at a laboratory angle of 27.5°. The solid (blue) histogram represents the experimental spectrum. The dashed lines are Geant 4 simulations including δ-electrons (black) and ISGMR (grey/red) reactions channels. The spectrum in the inset corresponds to a measurement without gas-jet (empty) target.

tracted. The number of counts in various strips would then produce angular distributions such as those shown in Fig. 6 from which information about GMR is extracted [22, 23]. With the help of a Multipole Decomposition Analysis (MDA), one can clearly see the dominance of $L = 0$ at the position where one expects the ISGMR to peak. Note the *very* small values of θ_{CM}. From this analysis, the peak position and the fraction of the Energy-Weighted Sum Rule has been obtained with the values in perfect agreement with the literature [24].
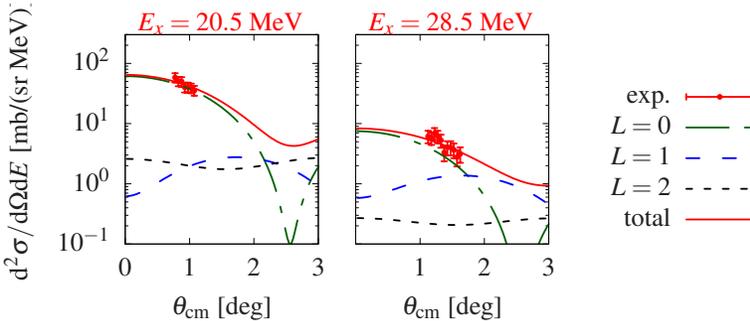

Fig. 6. Multipole-decomposition analysis (MDA) for ^{58}Ni. The two panels show angular distributions for two measured excitation energies.

The low value of θ_{CM} should be contrasted with the values obtained in an active target (which is around 4°) [25–27]. In fact, one will only be sensitive to the second maximum of the $L = 0$ component in those measurements.

5. Conclusions and outlook

For the first time, a nuclear reaction has been studied with a radioactive ion inside a storage ring. For the present measurement, much research and development has been done in order to have detectors operating at an ultra-high vacuum (UHV) environment. The results of this study show that not only these measurements are possible but also the performance of the detectors went beyond the specification. Measurements of the elastic cross section extended beyond the first minimum of the cross section allowing a precise measurement of the RMS matter radius with a preliminary value lying between 3.7 and 3.8 with a precision of 0.1 fm for ^{56}Ni. Since for the measurements of the giant monopole resonance higher luminosities would be required, the stable ^{58}Ni was chosen as the circulating beam. Also for this measurement, the precision obtained is extremely high allowing one to extract the parameters of the giant monopole resonance (ISGMR).

In order to perform measurements on ISGMR with radioactive ions, one either needs higher intensities or a larger coverage of the detector solid angle. In the forthcoming time, the plan of the collaboration is to increase the number of DSSDs inside the vacuum and cover a larger polar and azimuthal angle in the region where ISGMR becomes important. These measurements could still be carried out with the FRS beams at ESR.

In the longer run and once the Super-FRS beams with much higher intensities become available, one can either use HESR for experiments at high energies or use a return line to the ESR in order to work with lower energies. With either option, the detector will be equipped with many more detectors increasing the capabilities of the setup going to the design specifications as presented in Fig. 1.

REFERENCES

[1] www.fair-center.eu/public/experiment-program/nustar-physics.html

[2] www.fair-center.eu/public/experiment-program/nustar-physics/exl.html

[3] www.fair-center.eu/en/public/experiment-program/nustar-physics/r3b.html

[4] www.fair-center.eu/public/experiment-program/nustar-physics/elise.html

[5] M. Kühnel *et al.*, *Nucl. Instrum. Methods Phys. Res. A* **602**, 311 (2009).

[6] S. Ilieva, Ph.D. Thesis, University of Mainz, 2009.

[7] H. Moeini, Ph.D. Thesis, University of Groningen, 2010.

[8] S. Ilieva *et al.*, *Eur. Phys. J. Spec. Top.* **150**, 357 (2007).

[9] N. Kalantar-Nayestanaki *et al.*, *Int. J. Mod. Phys. E* **18**, 524 (2009).

[10] H. Moeini *et al.*, *Nucl. Instrum. Methods Phys. Res. A* **634**, 77 (2011).

[11] M. von Schmid *et al.*, *Nucl. Instrum. Methods Phys. Res. A* **629**, 197 (2011).

[12] B. Streicher *et al.*, *Nucl. Instrum. Methods Phys. Res. A* **654**, 604 (2011).

[13] M. Mutterer *et al.*, *Phys. Scr.* **2015**, 014053 (2015).

[14] Yu.A. Litvinov *et al.*, *Nucl. Instrum. Methods Phys. Res. B* **317**, 603 (2013).

[15] H. Reich *et al.*, *Nucl. Phys. A* **626**, 417 (1997).

[16] F. Nolden *et al.*, Proceedings of IPAC2013, 91, 2013.

[17] M. von Schmid, Ph.D. Thesis, Technische Univ. Darmstadt, 2015.

[18] M. von Schmid *et al.*, *Phys. Scr.* **2015**, 014005 (2015).

[19] H. Lenske, P. Kienle, *Phys. Lett. B* **647**, 82 (2007).

[20] A.N. Antonov *et al.*, *Phys. Rev. C* **72**, 044307 (2005).

[21] R.M. Tarbutton, K.T.R. Davies, *Nucl. Phys. A* **120**, 1 (1968).

[22] J.C. Zamora, Ph.D. Thesis, Technische Univ. Darmstadt, 2016.

[23] J.C. Zamora *et al.*, *Phys. Lett. B* **763**, 16 (2016).

[24] B.K. Nayak *et al.*, *Phys. Lett. B* **637**, 43 (2006).

[25] M. Vandebrouck *et al.*, *Phys. Rev. Lett.* **113**, 032504 (2014).

[26] M. Vandebrouck *et al.*, *Phys. Rev. C* **92**, 024316 (2015).

[27] S. Bagchi *et al.*, *Phys. Lett. B* **751**, 371 (2015).